Available online at www.sciencedirect.com
ScienceDirect
Physica B 395 (2007) 20–27
PHYSICA B
www.elsevier.com/locate/physb

Bias dependence of W, Mo and Ta conductance histograms

D. den Boer[a,*], O.I. Shklyarevskii[a,b], S. Speller[a]

[a]Institute for Molecules and Materials, Radboud University Nijmegen, Toernooiveld 1, NL–6525 ED Nijmegen, The Netherlands
[b]B. Verkin Institute for Low Temperature Physics and Engineering, National Academy of Science of Ukraine, 47 Lenin Avenue, 61103 Kharkov, Ukraine

Received 31 October 2006; received in revised form 10 January 2007; accepted 3 February 2007

Abstract

The increase of the bias voltage V_b above 0.4–0.5 V results in the emerging of new peaks in the conductance histograms of W, Mo and Ta. Only for Ta and for some of the Mo contacts these peaks are reproducible and related to stable atomic arrangements. For W the additional peaks are always contact specific. The shape of the conductance histogram at elevated V_b depends also on the bias voltage and is changing in the process of measurements for the majority of Mo contacts. Possible reasons for this non-typical behavior of conductance of molybdenum and tungsten nanocontacts are discussed.

PACS: 73.63.Rt; 73.40.Jn; 62.25.+g

Keywords: Break-junction; Nanocontact; Conductance; Bias; Tungsten; Molybdenum; Tantalum

1. Introduction

The conductance histogram technique was found to be an extremely useful tool to study the last stage of breaking a nanowire [1]. Since individual conductance traces measured in this process are inherently irreproducible, a statistical data analysis approach is of crucial importance. The field of application of this method is, however, much wider. It was employed to study one-atom chains in Au, Pt and Ir [2,3], electronic and atomic shell effects in the nanowires of single-valence metals [4,5], conductance through a hydrogen bridge between metallic electrodes [6,7] and the influence of hydrogen and oxygen on the conductance and length of atomic chains [8,9]. It turns out that conductance histograms are greatly influenced by the microstructure of the starting materials [10] and by the mechanical and the electronic properties of the electrode surface [11].

Histogram analysis on the bias dependence measurements of the conductance of gold [13,14] and aluminum [15,16] atom-sized contacts revealed the gradual suppression and disappearance of peaks. This effect was explained by the heating of the contact and by the current-induced instability at high V_b [17]. The other group of results on the high-bias contacts' stability and the non-ohmic behavior of the conductance was demonstrated in Refs. [18,19] using high-speed measurements of $I-V$ characteristics of gold and platinum contacts. Attempts to measure bias dependence of the conductance histogram for Pd, Pt, Rh, Ru and Ir [20,21] were limited by a conductance of approximately $3.5G_0$ and in the case of Pd and Ir demonstrated only the featureless dependencies. The evolution of the conductance of a single-atom platinum contact with the bias voltage up to 0.4 V was studied in Ref. [22].

Conductance histograms of many transition d-metals display only one peak corresponding to the conductance through a single-atom contact [1,11]. Most surprisingly we observed an emerging of extra peaks in conductance histograms of W, Mo and Ta mechanically controllable break-junctions (MCBJ) while studying the thermodesorption of dissolved hydrogen at elevated bias voltages [12]. The immediate question was what do these peaks relate to? To the presence of hydrogen atoms in the electrodes? To the additional stable atomic arrangements existing only at high V_b? Or do the peaks have a different origin? To

*Corresponding author. Tel.: +31 243652383.
E-mail address: d.denboer@science.ru.nl (D. den Boer).

0921-4526/$ - see front matter © 2007 Elsevier B.V. All rights reserved.
doi:10.1016/j.physb.2007.02.016

answer these questions we performed a systematic study of the voltage dependence of conductance histograms for W, Mo and Ta and we present it along with the possible models.

2. Experiment

We used a standard MCBJ technique described elsewhere [1] in our experiments. For the particular case of W, Mo and Ta most of details of sample preparation, characterization and measurements can be found in Ref. [11]. The sample mounting included two $6 \times 2.5 \times 1$ mm pieces of shear piezo-ceramic (which gives a horizontal displacement of its surface when voltage is applied) glued to the bending beam. Polycrystalline W, Mo or Ta wires with a diameter of $80-100\,\mu$m and a purity 99.95–99.99% were attached to the top of the piezo's (see Fig. 1 in Ref. [11]). The Mo and Ta wires were notched with a razor blade. To insure the break of the tungsten wire a deep notch was produced with a diamond saw. The wire was broken at 4.2 K in an ultra-high vacuum environment by bending the beam against the counter supports. The distance between the electrodes was fine tuned by changing the deflection of the bending beam or applying voltage to the shear piezo. The relative displacement of the electrodes was calibrated using the exponential part of $G(z)$ traces in the tunneling regime (assuming a work function for all materials $\phi \simeq 4.5$ eV) as well as by measuring field emission resonance spectra [23]. The contact conductance was measured by a current-to-voltage converter with a gain of $0.1-0.01\,\mathrm{V}/\mu\mathrm{A}$. Conductance traces for building conductance histograms were recorded with an NI PCI-6036E data acquisition board at sampling rate of 100 000 points/s. During this acquisition a ramp voltage (asymmetric triangle 2:98%) with a frequency of 10 Hz was applied to the shear piezo to establish a repeated fracture of the junction.

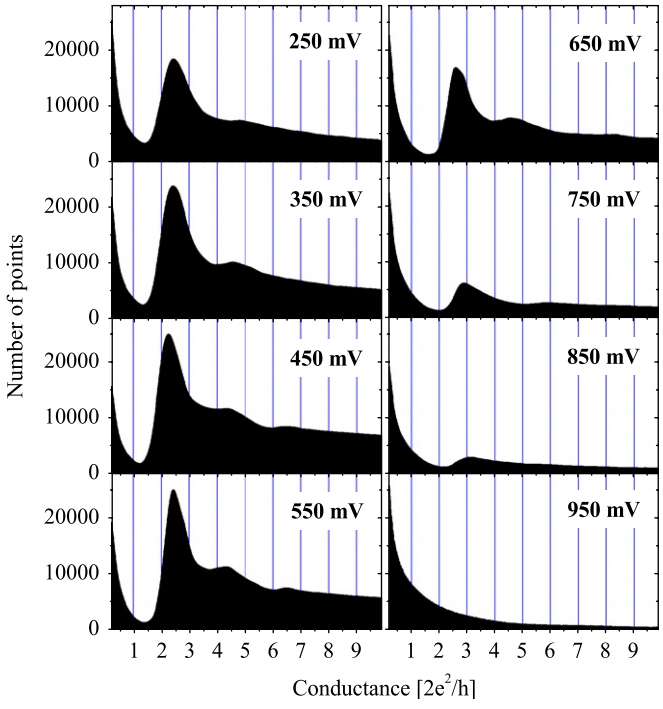

Fig. 1. Bias dependence of the Ta conductance histogram for V_b in the interval 250–950 mV. Each histogram was constructed from 10 000 individual conductance traces.

We thoroughly analyzed 80–100 conductance histograms for each of the metals measured for 3–5 different samples. The actual number of data was much larger, but it was extremely important to perform the complete cycle of measurements in the whole range of V_b (typically 0.1–1 V) for the *same* contact. This was imperative for W and Mo with the different processes of contact formation and break compared to ductile metals as will be described below. In the case of abrupt changes of contact parameters all previous data from this set were discarded.

3. Results and discussion

The conductance histograms for Ta have a typical bias dependence presented in Fig. 1. At bias voltages below 100 mV the conductance histograms for tantalum (as well as for molybdenum and tungsten) show a single peak in the range $2.3-2.5G_0$ related to the conductance through the single-atom contact (where $G_0 = 2e^2/h$ and $1/G_0 \approx 12.9\,\mathrm{k}\Omega$). Gradual increasing V_b leads to appearance of the second peak at $4.5G_0$. The third peak around $6.5G_0$ was observed only in a limited range of bias voltages (400–600 mV). At $V_b \geqslant 600$ mV the rapid degradation of these peaks is starting and culminating in the total disappearance of all features at $V_b \geqslant 900$ mV. In view of what follows it should be especially noted that with insignificant variation in the peak shapes, position and their relative amplitudes the overall picture remains practically the same for all contacts studied. At bias voltages exceeding 1000 mV we found that contact parameters are changing rapidly with the subsequent snapping together of electrodes to the low ohmic contact or with complete disconnections outside the reach of the piezo-driver.

Since all histograms presented in Fig. 1 were taken for the same contact and contain the same number of conductance traces, it is possible to do a quantitative analysis of the data. The dependence of the number of data points per conductance trace in the range from 1 to $9.9G_0$ (or the "pulling length") on V_b is presented in Fig. 2. This curve reaches its maximum between 400 and 500 mV and then drops almost by an order of magnitude at 900 mV. To compare our results with those for Au and Al [14,16] we also calculated the length of the conductance "plateau" for the first peak L_p^1. To this end we summed up all data points in the range of conductances from $0.9G_{max}^1$ to $1.1G_{max}^1$ where G_{max}^1 is the position of the first conductance maximum. Dividing this quantity by the total number of conductance traces per histogram we found the number of data points per single conductance trace. Subsequently, we

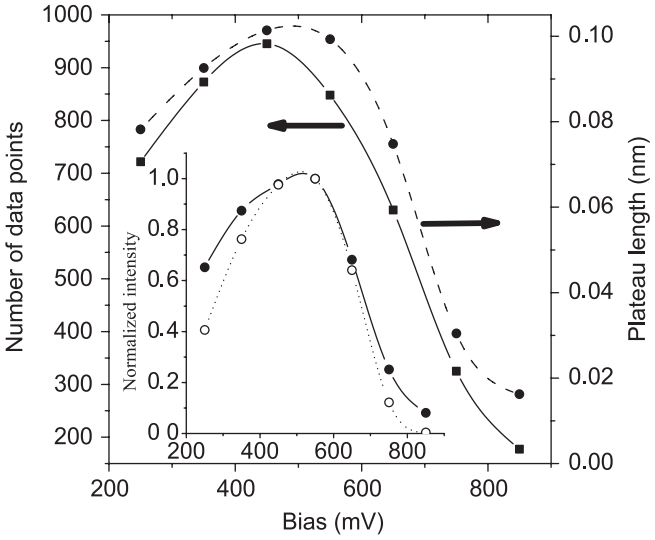

Fig. 2. The average number of data points for a single conductance trace (from 1 to $9.9G_0$) for histograms presented in Fig. 1 and the length of plateau for the one-atom contact taken in conductance window $0.9G^1_{max}$ to $1.1G^1_{max}$ (dashed curve). Inset: the normalized intensity of the first (solid line) and the second peak (dashed line) for the same histograms.

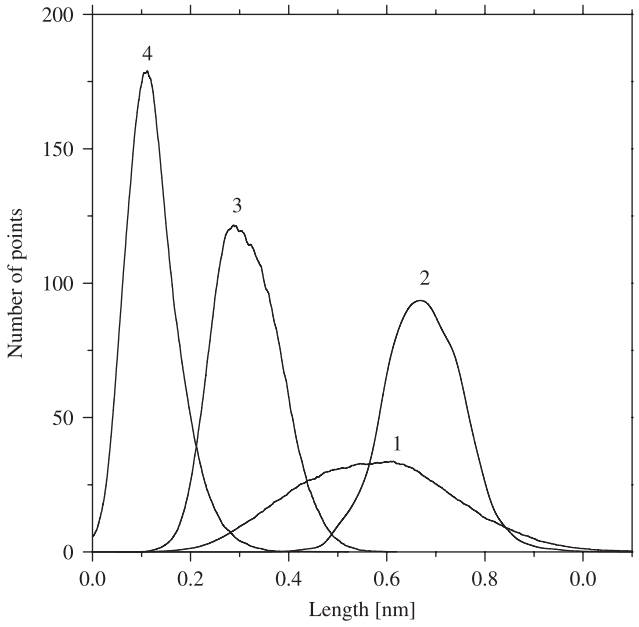

Fig. 3. Histograms for the total length of conductance traces (taken in the range $1-9.9G_0$) measured for 25 000 traces at bias voltages: 1—300 mV; 2—500 mV; 3—700 mV and 4—900 mV.

used the calibration coefficient for the shear piezo to plot the dependence of L^1_p on V_b (dashed curve in Fig. 2). The width of conductance window for the first plateau was chosen more or less arbitrarily. Increasing its width to 0.8–1.2 of G^1_{max} or using the fixed conductance window of $1.0G_0$ yields similar behavior of the $L^1_p(V_b)$ dependence (with a larger value of L^1_p). At $V_b > 700$ mV, the contribution of the featureless conductance traces to the "background" could not be ignored and was subtracted.

The distribution of the total length of individual conductance traces can be obtained from the measurements in a way similar to the length histogram method for single-atom gold chains [2] (with data points taken in the range $1-9.9G_0$). The results of such measurements are presented in Fig. 3 for 25 000 traces in each histogram. Apart from the predictable behavior of the position of the maximum we observed the narrowing of the length distribution. In all cases (except curve 4) the shape of it remains perfectly Gaussian. At bias voltages $\geqslant 900$ mV the main reason for deviation of the curves from the Gaussian distribution is the ever increasing number of the traces with "zero length" related to the abrupt jump from the low ohmic contact to tunneling.

The dependencies demonstrated above are in a qualitative agreement with previous experiments on ductile metals [14,16]. The major difference, however, is the appearance of additional peaks in the conductance histograms. This effect is directly related to heat dissipation within the contacts at high bias voltages accompanied by the increase of the temperature. Additional peaks can be observed only in the limited range of V_b as the further increase of the bias voltage (and consequently the temperature and current-induced forces) results in the rapid degradation of all the features in the histograms.

To estimate the temperature inside the contact is one of the most difficult problems. In the case when both the elastic and the inelastic mean free paths are considerably less than the contact diameter d, the so-called thermal limit, there is a linear dependence between the applied bias voltage and the temperature in the center of the contact, $eV = 3.63k_BT$ [24]. This formula gives us an unrealistic 3000 K at ~1 V. Estimations of Todorov et al. [25] made for Au single-atom contacts and chains yield a considerably lower overheating above the ambient temperature. However, the applicability of these results to the refractory d-metals is highly questionable. In case of the solid solution of hydrogen in Ta, Mo and W, the large scattering of conductance electrons on the protons brings the situation close to the thermal limit [12]. Comparing the conductance histograms with thermodesorption spectra of hydrogen measured by other methods we found that at a bias voltage of 300–400 mV the temperature inside the contact is in the range of 400–700 K or approximately two times less than calculated for the "true" thermal limit. For pure Ta this figure is supposed to be even smaller, but overheating the center of the contact at $V_b \sim 800-900$ mV to 700–1000 K would not be a surprise, when one takes into account the scattering on the defects and on the interface between the electrodes. At the maximum conductance that is reached by the contact, during the formation process ($50-100G_0$) the power dissipation around the nanoconstriction is $\approx 5-10$ mW. This is quite enough for the overheating mentioned above.

In BCC metals the plastic flow is governed by the overcoming of the Peierls barriers. Therefore, the yield

stress of the BCC metals is strongly temperature dependent and decreases considerably with increase of the temperature in contrast to the FCC materials. This increases the mobility of the atoms in the connective neck between the electrodes and enables or greatly enhances their probability to form the stable two- and three-atom configurations in the process of contact evolution. Another reason for appearance of the second (and third) peaks is the reduction of the background level of the histograms. The smeared structure around $4-5G_0$ in the conductance histograms of Ta was on some occasion even visible at $V_b = 100\,\text{mV}$ and a well-defined second peak was at low biases observed in the conductance histograms of BCC Nb and V by Yanson [26]. Presumably, the largest contribution to the background is coming from the short conductance traces. Increase of the conductance traces' length with V_b and simultaneous narrowing of the conductances traces' length distribution (curves 1 and 2 in Fig. 3) may indicate the reduction of the background level. However, the concept of the "background" of conductance histogram by itself is not well established so far. One can claim that the featureless histograms (e.g. histograms for Ta taken at 900 mV, Fig. 1) is representing the "pure" background. This is certainly not true for the rest of the conductance histograms presented in Fig. 1 since the level of background increases again at larger G, after reaching its minimum around $1.5G_0$. The simplest assumption in our case is that the background in this range is a monotonically increasing function. To compare the bias dependence of the intensity of the first and the second peak we suggested and subtracted the linearly increasing background. The results for normalized intensities of these peaks are presented in the inset in Fig. 2. Stronger bias dependence of the intensity of the second peak indicates that although the contribution of the background reduction in the emergence of the second peak should not be neglected, the main reason for this effect is the enhanced mobility of the Ta atoms in the connective neck. In our previous experiments with tungsten MCBJ we chemically etched the W wire down to a $\sim 5\,\mu\text{m}$ thick neck to initiate the break. For this type of electrodes we observed either featureless histograms or we observed peaks related to the conductance through the $5d_{z^2}$ dangling-bond surface states when the break of tungsten wire occurs along the W(0 0 1) plane [11]. With a mechanically produced notch it has become possible to measure histograms with a one-atom peak with a conductance close to $2.5G_0$.

At first sight the dependence of the conductance histograms on the bias voltage for W (Fig. 4) has many features similar to the dependencies presented above for Ta. The amplitude of the histogram peaks, the length of the conductance traces and the first plateau are increasing with V_b (Fig. 5) with a subsequent decrease at $V_b \geqslant 700\,\text{mV}$, although the variation of these quantities is much smaller than for Ta. The series of additional peaks appears at $V_b \approx 700\,\text{mV}$ and remains partly visible even after the total disappearance of the first peak at $V_b \geqslant 1000\,\text{mV}$.

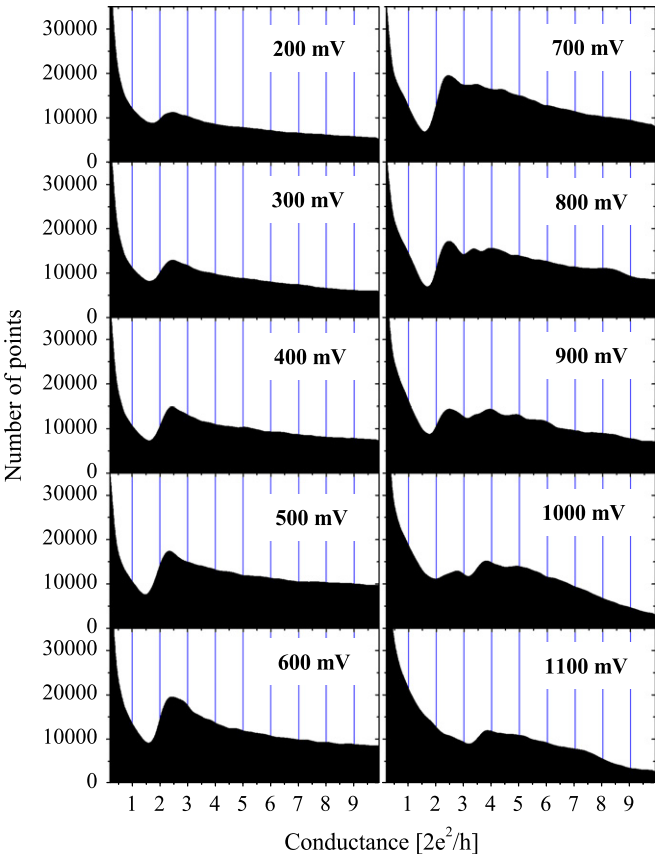

Fig. 4. Bias dependence of the W conductance histogram for V_b in the range 200–1100 mV. Each histogram was constructed from 10 000 individual conductance traces.

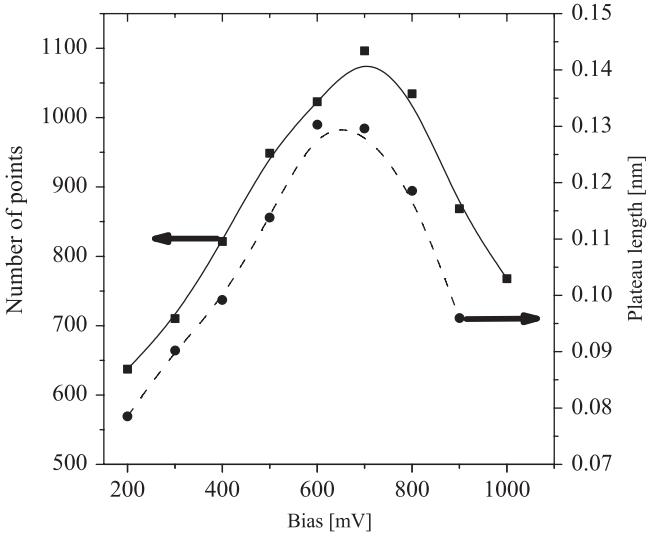

Fig. 5. The average number of data points for a single conductance trace (from 1 to $9.9G_0$) for W histograms presented in Fig. 3 and the length of plateau for the one-atom contact taken in conductance window $0.9G^1_{max}$ to $1.1G^1_{max}$ (dashed curve).

While measuring conductance histograms for different contacts at $V_b = 700\,\text{mV}$ we found a vast variation of the positions and the amplitudes of the additional peaks

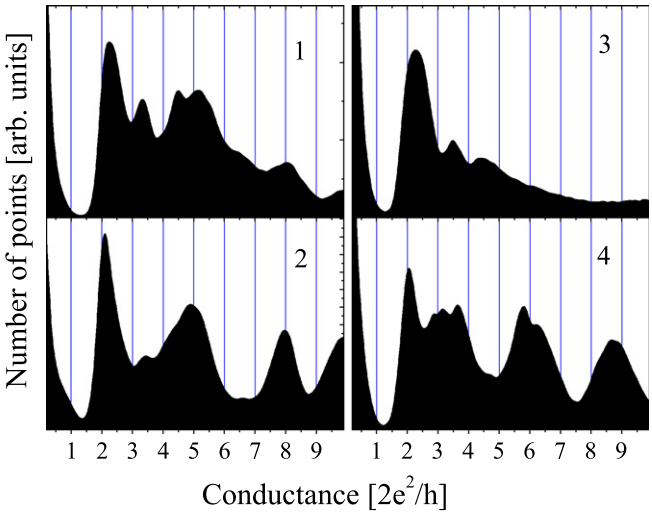

Fig. 6. Conductance histograms for different W contacts measured at 700 mV.

(Fig. 6). Histograms 1 and 2 bear a certain resemblance because they were measured for practically the same contact with only one of the parameters of experiment slightly changed—the amplitude of the ramp voltage applied to the shear piezo and therefore the "indenting" of the electrodes.

It is quite evident that the reason of the unusual behavior of the conductance histograms for tungsten at elevated bias voltages is related to the different process of the contact formation and break as compared to the ductile metals. The elastic module of tungsten (shear modulus $G = 160$ GPa and Young's modulus $E = 410$ GPa) are extremely large even compared to those of Ta ($G = 69$ GPa and $E = 186$ GPa). Before discussing the possible models at length we would like to demonstrate the results of our measurements for molybdenum MCBJ. This metal has the elastic module of $G = 120$ GPa and $E = 330$ GPa, so exactly in between the values for Ta and W.

The typical set of data for the bias dependence of Mo conductance histograms is presented in Fig. 7. The additional peaks in this case are already emerging at $V_b \approx 400$ mV, but in contrast to the tungsten contacts these peaks are not reproducible at higher bias voltages and are replaced by a completely new row of peaks at V_b 500, 600 and 700 mV. For this type of contacts no measurements at bias voltages exceeding 700 mV were possible. Conductance histograms for different contacts at the same bias voltage (Fig. 8) demonstrate no common features (except the first peak). The histogram number 4 in Fig. 8 is a cumulative one and was constructed from 40 individual histograms (containing altogether about 500 000 conductance traces) measured at $V_b = 500$ mV for different contacts, different samples and at different dates. It demonstrates only the first peak accompanied by the nearly flat background. This proves that the position of the newly emerging peaks can be completely random.

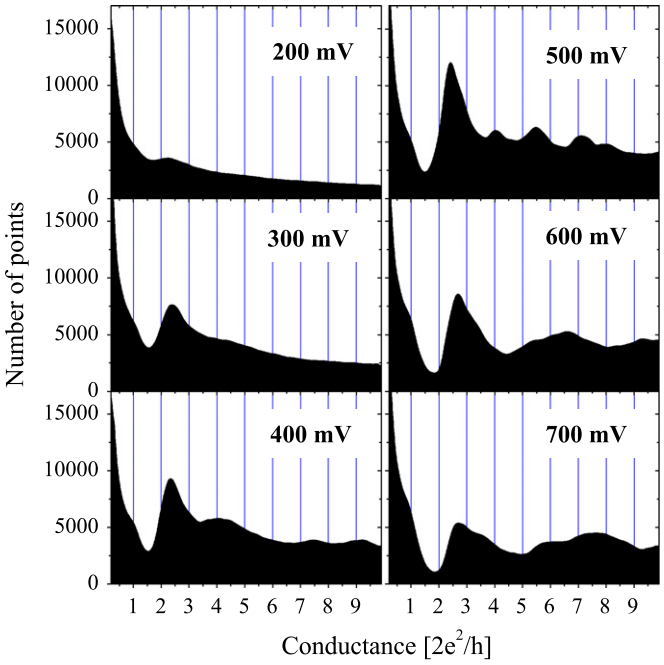

Fig. 7. The typical set of conductance histograms for Mo in the range of bias voltages from 200 to 700 mV.

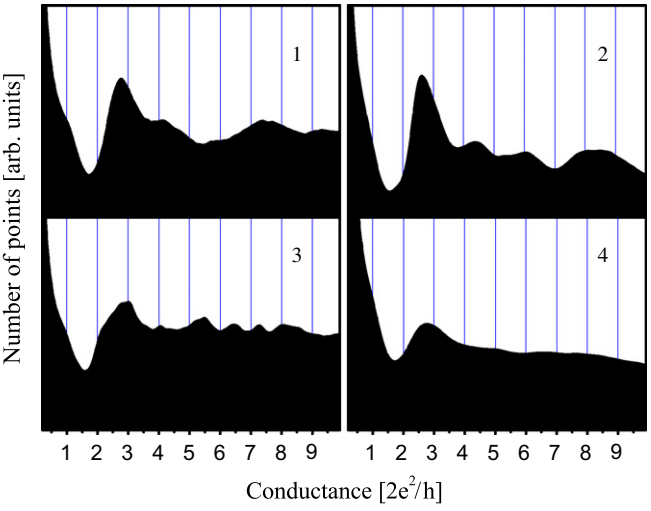

Fig. 8. 1–3—Conductance histograms for different Mo contacts measured at 500 mV. 4—Cumulative histogram made of 40 histograms (500 000 individual traces) measured for different samples.

Conductance histograms for Mo not only tend to change with bias voltage but also undergo considerable changes at the same voltage in the course of the measurements. Conductance histograms in Fig. 9 were measured in succession for the same contact without any changes in the parameters of the experiment. During this time (approximately 1 h for the whole set) the shape, amplitude and position of the peaks have changed drastically.

On some occasions the conductance histograms of Mo demonstrate different behavior presented in Fig. 10. In the range 400–600 mV we observed the emerging of two weak

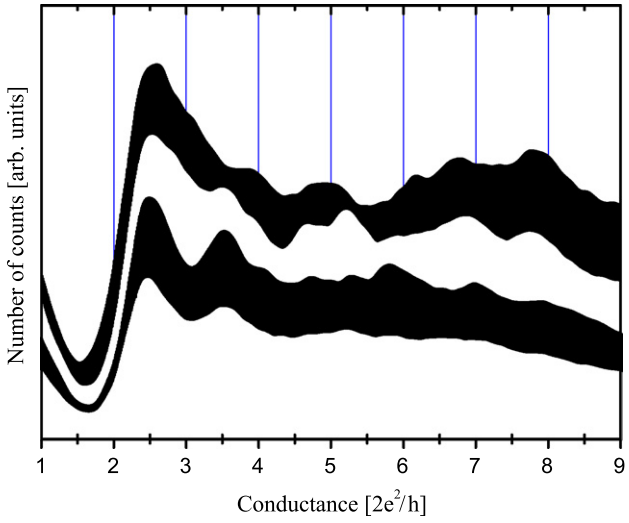

Fig. 9. Time evolution of the conductance histograms for Mo at 500 mV (from the bottom to the top). All measurements were done in succession within approximately 1 h.

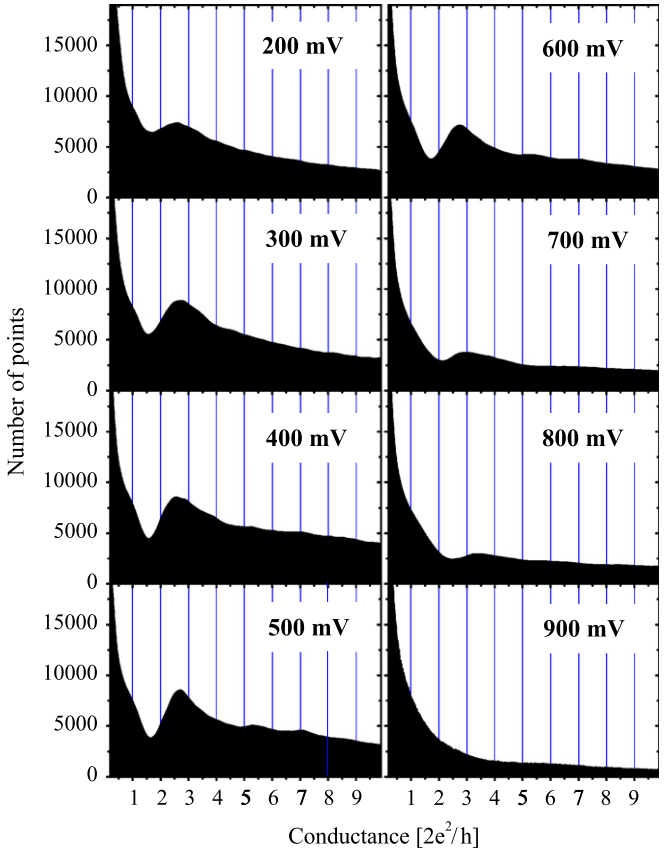

Fig. 10. The alternative set of conductance histograms for Mo with reproducible peaks at 5.2 and $7.2G_0$ emerging in the range of bias voltages of 500–600 mV.

peaks at conductances $\sim 5G_0$ and $7G_0$. These peaks were fairly reproducible and did not change their position with time or bias voltage. Therefore, they can be regarded as related to the stable and reproducible atomic arrangements in the connective neck between the electrodes. Our data for Mo show that this metal demonstrates features common either to Ta or to W depending on the specific contact and therefore on the electrodes local topography and crystallographic orientation with respect to their axis.

In ductile metals the junction breaks through the process of rupture. Conductance traces show a stepwise behavior with plateaus corresponding to stable atomic configurations. The sudden jumps are due to the force relaxation accompanied by the transition to the next stable arrangement of atoms in the contact [27]. In the stable configurations the deformation is elastic and reversible while relaxation of the stress means plastic deformation within a few neighboring atomic layers. The numerous attempts of molecular dynamic simulation of this process are reviewed in detail in Ref. [1].

In case of brittle materials with a large elastic modulus and spring constant (like tungsten and some conducting ceramics [28]) the picture described above is not applicable. For the stiff geometry of the electrodes the formation and break of the contact may occur through the sliding motion of electrode surfaces with respect to each other with either no or insignificant indenting. We found some evidence for this suggestion while measuring the dependence of the tunnel current on the piezovoltage V_p. The scattering in the slope of $\log I(V_p)$ curves indicates that on many occasions one of the electrodes is approaching another along the tangent curve.

Additional peaks in conductance histograms, however, are not related directly to geometrical effects such as relief of the electrodes surface (''wash-board'' effect) as it does not suggest any temperature dependence. In fact, the detectable changes in the slope of the conductance traces, related to the surface relief of the electrodes, occur on the scale $\sim 10-20G_0$ or approximately 1–2 nm in real space and result in the variation of the amplitude of the background in histograms at the same scale.

Recently, the effects of pseudoelastic deformation and shape memory in nanowires have drawn considerable attention [29,30]. The partial reproducibility of stress–strain dependencies suggests the repeatable features in the conductance curves. However, these effects are restricted to the FCC nanowires and related to the $\langle 1\,0\,0\rangle$ to $\langle 1\,1\,0\rangle/\{1\,1\,1\}$ reorientation process.

Analysis of nanowire stability at high voltages performed in Ref. [31] revealed the existence of geometries that are stable only under an applied bias. This, however, suggests reproducible features in the conductance histogram which is not the case in our experiments.

Additional peaks in Mo and W histograms can be explained by plastic deformation of these materials at elevated temperatures where the yield strength is greatly reduced. During sliding motion the mutual orientation between the direction of the applied stress, the contact axis and the crystallographic axis of the deformed material is changing constantly. (For highly textured tungsten wires the [1 1 0] direction is almost always parallel to the contact

axis). Taking into account 48 possible slip systems for BCC metals, we are facing a very complicated process that controls the succession of atomic arrangements in the neck during stress relaxation. The degree of the neck deformation depends on the local relief of the surfaces of the electrodes. This makes neck evolution contact specific and explains why a slight increase of the electrode indenting results in drastic changes in the histograms (see histograms 1 and 2 in Fig. 6). Nevertheless, the emerging of new peaks proves that even when the connective neck is heavily deformed some atomic configurations are more stable than others.

For Mo that has a relatively low melting point (as compared to W and Ta) the constant modification of the electrode surfaces due to the electromigration of atoms during measurements and the increase of V_b is possible. Accordingly, this leads to the observed changes in the histogram shape (Figs.7 and 9). For some geometries of the electrodes the sliding motion is prohibited and formation and break of the contact occur in the same way as for ductile materials leading to the reproducible peaks in the conductance histograms (Fig. 10). The role of the temperature in the observed effect should be emphasized once more. On measuring the *return* histograms we did not observe the appearance of extra peaks at high V_b. In this case the data are related to the still cold and virtually not plastically deformed electrodes.

For all materials studied we observed a displacement of the first peak in the histograms toward higher G as the bias voltage increased. The typical dependencies of the position of the first peak on V_b are shown in Fig. 11. For transition d-metals five conductance channels are expected to contribute to the conductance of a single-atom contact, according to the number of valence orbitals. The transmission values of these conductance channels were studied for single-atom niobium junctions by tight binding calculations [32] and by measuring a subgap structure in the superconducting state [33]. Our results indicate that the transmission of at least some of the channels increase significantly at voltages above 500–700 mV.

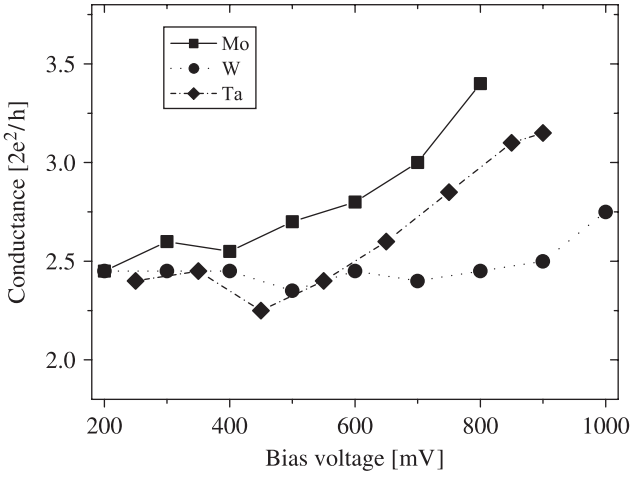

Fig. 11. Dependence of the first peak position on the bias voltage for Ta, Mo and W. Data are taken from the histograms presented in Figs. 1, 4 and 10.

Experimental study of the $I-V$ curves of atomic-sized Pt contacts revealed their non-linear behavior (substantial decrease in conductance) at $V_b \geqslant 400$ mV [19]. However, there is no contradiction between these results and our data because, as was pointed out in Ref. [19], the complex valence electron structure for metals with open d shells usually results in complex behavior of transmission through the individual channels with V_b. This in turn may result both in decrease and increase in the total transmission of conductance channels.

4. Conclusions

We observed the appearance of extra peaks in the conductance histograms of W, Mo and Ta at bias voltages exceeding 0.4–0.5 V. For Ta and some of the Mo contacts these peaks are fairly reproducible and are related to stable atomic configurations. For W additional peaks are reproducible in the whole range of the bias voltages only for the same contact, but their number, position and amplitude are varying from contact to contact. Finally, for most of the Mo junctions the overall shape of conductance histograms is changing with bias voltages and in the course of time in the process of measurement. We suggested that the origin of these peaks is related to the different types of formation and breaking of the contacts for metals with large elastic modulus. Instead of indenting, the surfaces of the electrodes are sliding with respect to each other. At low V_b this results either in a featureless conductance histogram [11,20] or in histograms with a peak corresponding to the single-atom contact. At elevated bias voltages the temperature in the contact may easily reach 500–1000 K reducing the elastic modulus of the material. For Ta this enables new stable atomic configurations in the process of breaking the connective neck between electrodes. The contribution of the reduction of the background in the emergence of the extra peaks at elevated V_b should not be underestimated as well. For W and Mo the sliding motion of electrodes leads to the complex character of the plastic deformation of electrodes depending on the relative orientation of the direction of applied stress and crystallographic axis of the metals. During the process of the electrode disconnection, the conductance of the contact will be influenced by the details of the relaxation processes related to the local shape of the electrodes. Although the suggested model is extremely tentative it gives a consistent explanation of the observed effects which are itself of considerable practical interest.

Acknowledgments

The authors are grateful to A.J. Toonen, J. Hermsen and J. Gerritsen for invaluable technical assistance. Part of this work was supported by the Nanotechnology initiative of

the Netherlands NanoNed and the Stichting voor Fundamenteel Onderzoek der Materie (FOM) which is financially supported by the Nederlandse Organisatie voor Wetenschappelijk Onderzoek (NWO). O.I.S. wishes to thank the FOM and NWO for a visitor's grant.

References

[1] N. Agrait, A.L. Yeyati, J.M. van Ruitenbeek, Phys. Rep. 377 (2003) 8103.
[2] A.I. Yanson, G.R. Bollinger, H.E. van den Brom, N. Agraït, J.M. van Ruitenbeek, Nature (London) 395 (1998) 783.
[3] R.H.M. Smit, C. Untiedt, A.I. Yanson, J.M. van Ruitenbeek, Phys. Rev. Lett. 87 (2001) 266102.
[4] A.I. Yanson, I.K. Yanson, J.M. van Ruitenbeek, Nature (London) 400 (1999) 144.
[5] A.I. Mares, A.F. Otte, L.G. Soukiassian, R.H.M. Smith, J.M. van Ruitenbeek, Phys. Rev. B 70 (2004) 073401.
[6] R.H.M. Smit, Y. Noat, C. Untiedt, N.D. Lang, M.C. van Hemert, J.M. van Ruitenbeek, Nature 419 (2002) 906.
[7] Sz. Csonka, A. Halbritter, G. Mihaly, E. Jurdik, O.I. Shklyarevskii, S. Speller, H. van Kempen, Phys. Rev. Lett. 93 (2004) 016802.
[8] Sz. Csonka, A. Halbritter, G. Mihaly, E. Jurdik, O.I. Shklyarevskii, S. Speller, H. van Kempen, Phys. Rev. Lett. 90 (2003) 116803.
[9] W.H.A. Thijssen, D. Marjenburgh, R.H. Bremmer, J.M. van Ruitenbeek, Phys. Rev. B 96 (2006) 026806.
[10] I.K. Yanson, O.I. Shklyarevskii, Sz. Csonka, H. van Kempen, S. Speller, A.I. Yanson, J.M. van Ruitenbeek, Phys. Rev. Lett. 95 (2005) 256806.
[11] A. Halbritter, Sz. Csonka, G. Mihaly, E. Jurdik, O.Yu. Kolesnychenko, O.I. Shklyarevskii, S. Speller, H. van Kempen, Phys. Rev. B 68 (2003) 035417.
[12] D. den Boer, O.I. Shklyarevskii, J.A.A.W. Elemans, S. Speller, J. Phys. Conf. Ser., accepted for publication.
[13] H. Yasuda, A. Sakai, Phys. Rev. B 56 (1997) 1069.
[14] K. Itakura, K. Yuki, S. Kurokawa, H. Yasuda, A. Sakai, Phys. Rev. B 60 (1999) 11163.
[15] J. Mizobata, A. Fujii, S. Kurokawa, A. Sakai, Jpn. J. Appl. Phys. 42 (2003) 4680.
[16] J. Mizobata, A. Fujii, S. Kurokawa, A. Sakai, Phys. Rev. B 68 (2003) 155428.
[17] Z. Yang, M. Chshiev, M. Zwolak, Y.-C. Chen, M. Di Ventra, Phys. Rev. B 71 (2005) 041402.
[18] K. Hansen, S.K. Nielsen, M. Brandbyge, E. Lægsgaard, F. Besenbacher, Appl. Phys. Lett. 77 (2000) 708.
[19] S.K. Nielsen, M. Brandbyge, K. Hansen, K. Stokbro, J.M. van Ruitenbeek, F. Besenbacher, Phys. Rev. Lett. 89 (2002) 066804.
[20] K. Itakura, H. Yasuda, S. Kurokawa, A. Sakai, J. Phys. Soc. Japan 69 (2000) 625.
[21] K. Yuki, S. Kurokawa, A. Sakai, Jpn. J. Appl. Phys. 40 (2001) 803.
[22] S.K. Nielse, Y. Noat, M. Brandbyge, R.H.M. Smit, K. Hansen, L.Y. Chen, A.I. Yanson, F. Besenbacher, J.M. van Ruitenbeek, Phys. Rev. B 67 (2003) 245411.
[23] O.Yu. Kolesnychenko, O.I. Shklyarevskii, H. van Kempen, Rev. Sci. Instrum. 70 (1999) 1442.
[24] Y.G. Naidyuk, I.K. Yanson, Point Contact Spectroscopy, Springer, New York, 2004.
[25] T.N. Todorov, J. Hoekstra, A.P. Sutton, Phys. Rev. Lett. 86 (2001) 3606.
[26] A.I. Yanson, Ph.D. Thesis, University of Leiden, 2001.
[27] G. Rubio, N. Agraït, S. Viera, Phys. Rev. Lett. 76 (1996) 2302.
[28] F. Ott, S. Barberan, J.G. Lunney, J.M.D. Coey, P. Berthet, A.M. de Leon-Guevara, A. Revcolevschi, Phys. Rev. B 58 (1998) 4656.
[29] H.S. Park, K. Gall, J.A. Zimmerman, Phys. Rev. Lett. 95 (2005) 255504.
[30] W. Liang, M. Zhou, Phys. Rev. B 73 (2006) 115409.
[31] C.-H. Zhang, J. Bürki, C.A. Stafford, Phys. Rev. B 71 (2005) 235404.
[32] J.C. Cuevas, A.L. Yeyati, A. Martín-Rodero, Phys. Rev. Lett. 80 (1998) 1066.
[33] B. Ludoph, N. van der Post, E.N. Bratus, E.V. Bezuglyi, V.S. Shumeiko, G. Wendin, J.M. van Ruitenbeek, Phys. Rev. B 61 (2000) 8561.